

# Free-space lossless state-detection of a single trapped atom

A. Fuhrmanek, R. Bourgain, Y.R.P. Sortais, and A. Browaeys

*Laboratoire Charles Fabry, Institut d'Optique, CNRS, Univ Paris-Sud,  
Campus Polytechnique, 2 avenue Augustin Fresnel, RD 128, 91127 Palaiseau cedex, France*

(Dated: May 22, 2018)

We demonstrate the lossless state-selective detection of a single rubidium 87 atom trapped in an optical tweezer. This detection is analogous to the one used on trapped ions. After preparation in either a dark or bright state, we probe the atom internal state by sending laser light that couples an excited state to the bright state only. The laser induced fluorescence is collected by a high numerical aperture lens. The single-shot fidelity of the detection is  $98.6 \pm 0.2\%$  and is presently limited by the dark count noise of the detector. The simplicity of this method opens new perspectives in view of applications to quantum manipulations of neutral atoms.

PACS numbers: 37.10.Gh, 03.67.-a, 32.80.Qk

Cold and trapped neutral atoms and ions are model systems to explore quantum computation [1–3] and quantum simulation of many-body systems [4, 5]. They are also the basis of a variety of entangled states that open new and exciting perspectives for quantum metrology [6]. For all these applications one requires in particular the control of the internal states on which quantum information is encoded. This can be done by using laser manipulation techniques. Another important requirement is the ability to read the internal state of the atoms or ions with a high fidelity and a minimal loss probability after performing a quantum manipulation.

A widely used method for state detection relies on fluorescence measurement [7]. To do so, one identifies a bright and a dark state, which can be e.g. two hyperfine ground states, separated by several GHz typically. The bright state is coupled to an excited state by a closed optical transition. The signature of the bright state population is the emission of fluorescence light by the atom or ion when it is illuminated by a probe laser tuned to this transition. The signature of the dark state population, on the contrary, is the absence of fluorescence due to the large hyperfine splitting. As this method relies on photon scattering, the energy of the probed atom or ion increases with the number of recoils. In the case of ions, traps depths of several thousands of Kelvins are typical, leading to a very efficient state detection with a negligible loss probability. There, detection fidelities as high as 99.99% have been reported [8].

Neutral atoms are also considered as forefront candidates for sophisticated quantum operations as one can handily control their interactions [9–12]. They also provide built-in scalability when placed in optical lattices [2]. However, the detection technique mentioned above, when applied to neutral atoms, is hampered by the small trap depth, typically lower than a few milliKelvins. The heating induced by the probe laser leads more easily to the loss of the atom before one can collect enough photons to decide in which state the atom is. Many groups have therefore implemented a so-called “push-out” measure-

ment based on the state-selective loss of the atom when it is illuminated by a resonant laser [13–15]. Although this technique has been proved to be efficient and quantum projection limited [15], it does not discriminate between detection induced losses from any other unwanted losses. One is therefore in demand of a detection scheme that is not based on the atom loss.

One way to implement lossless and yet efficient detection is to place the trapped atom in an optical cavity. Thanks to the Purcell effect, the fluorescence rate is enhanced in the cavity mode such that enough fluorescence photons can now be collected without losing the atom. Recently, two experiments demonstrated the state selective detection of a single atom using an optical cavity with reported fidelities larger than 99.4% [16, 17].

In another approach one can simply make use of a lens with a high numerical aperture to collect the fluorescence emitted by an atom trapped in an optical dipole trap. In this Letter, we follow this route and demonstrate the single-shot detection of the internal state of a rubidium 87 atom trapped in an optical tweezer. The fidelity of this state selective detection method is 98.6% in 1.5 ms and the probability to lose the atom during the detection is less than 2%.

The bright state used in our experiment is the hyperfine Zeeman state  $|\uparrow\rangle = |5S_{1/2}, F = 2, M = 2\rangle$  (see Fig. 1a). It is coupled to the excited state  $|e\rangle = |5P_{3/2}, F' = 3, M = 3\rangle$  by a closed transition at  $\lambda = 780$  nm. The dark state can be any Zeeman state of the  $(5S_{1/2}, F = 1)$  manifold, including  $|\downarrow\rangle = |5S_{1/2}, F = 1, M = 1\rangle$  [23]. It is separated from the bright state by  $\sim 6.835$  GHz. Let us estimate the feasibility of the state detection, using probe light tuned to the transition between  $|\uparrow\rangle$  and  $|e\rangle$  (the line width is  $\Gamma/2\pi = 6$  MHz and the saturation intensity is  $I_{\text{sat}} = 1.67$  mW.cm $^{-2}$ ). To do so, we consider an atom prepared at the bottom of the dipole trap in state  $|\uparrow\rangle$  and we estimate the number of absorption-spontaneous emission cycles that elevate the energy of the atom by an amount equal to the trap depth  $U$ . For  $U/k_B = 2$  mK (typical value for our experiment;

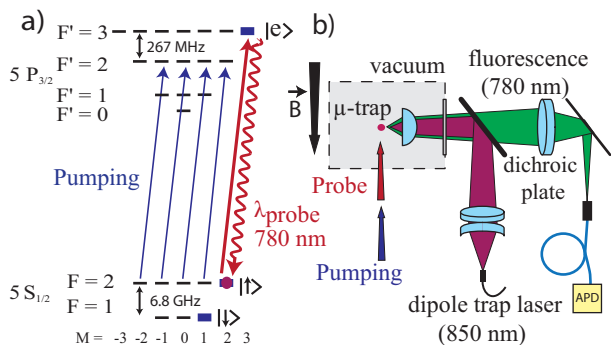


Figure 1: (Color online) *a*) Energy diagram of the D2 line of  $^{87}\text{Rb}$ . *b*) Experimental set-up. An aspheric lens focuses a 850 nm laser beam down to a spot with a  $1.1 \mu\text{m}$  waist ( $\mu$ -trap). Resonant probe light induces the fluorescence of a single atom loaded in the microscopic trap, which we detect on a fibered avalanche photodiode (APD).

$k_B$  is the Boltzmann constant), this number is on the order of  $U/2E_r \approx 5000$  ( $E_r = \frac{\hbar^2 k^2}{2m}$  is the recoil energy induced by a photon with a wave vector  $k = 2\pi/\lambda$ ,  $m$  is the mass of the atom). This number puts constraints on the probe light parameters in order to detect the atom without losing it. Taking for the saturation parameter  $s = I/I_{\text{sat}} = 0.1$  and for the probe duration  $\Delta t = 1$  ms yields a number of scattered photons  $\frac{I}{2} \frac{s}{1+s} \Delta t \sim 2000$  during the probe pulse, below the 5000 photons calculated above. Using an imaging system with a detection efficiency of 0.6% [18], one thus expects to detect  $\sim 11$  fluorescence photons in 1 ms. As our noise level is well below 1 photon during this time, the bright state  $|\uparrow\rangle$  should be identified unambiguously. Based on this estimation we have implemented this method on a single atom.

Our experimental setup, represented in Fig. 1b), has been described in detail elsewhere [19]. A single atom is trapped in an optical tweezer produced by a linearly polarized 850 nm laser. The optical tweezer is obtained by sharply focusing the laser through an aspheric lens with a numerical aperture of 0.5. The atom is captured from an optical molasses and due to the small trapping volume only one atom is trapped at a time [19]. The temperature of the atom, measured by a release-and-recapture technique [20], is  $35 \mu\text{K}$  in a 2.2 mK deep trap. This value ensures that the atom is close to the bottom of the trap. We collect the fluorescence light emitted by the atom using the same aspheric lens. This light is detected by a fibre coupled avalanche photodiode operating in a single photon counting regime. At the beginning and at the end of each sequence (see below), we test the presence of the atom in the trap by collecting the fluorescence light induced by the molasses beams. To detect the internal state of the atom, we send a unidirectional  $\sigma^+$ -polarized probe laser propagating along the quantization axis and tuned to the transition from  $|\uparrow\rangle$  to  $|e\rangle$ . The quantization

axis is set by applying a magnetic bias field of 1 G.

The experimental sequence begins with a single atom in a 2.2 mK deep trap. After switching off the molasses lasers we start the preparation phase in the bright state. We decrease adiabatically the trap depth down to 0.24 mK and turn on the bias field. The state preparation is achieved through optical pumping by sending a  $500 \mu\text{s}$  pulse of pumping light tuned to the transition ( $5S_{1/2}, F = 2$ ) to ( $5P_{3/2}, F' = 2$ ) superimposed to repumping light tuned to the transition ( $5S_{1/2}, F = 1$ ) to ( $5P_{3/2}, F' = 2$ ). Both laser beams propagate along the quantization axis and are  $\sigma^+$ -polarized. We measure the fidelity of the preparation in ( $5S_{1/2}, F = 2$ ) by using the “push-out” technique mentioned in the introduction. We find a hyperfine state preparation efficiency of 99.97%, obtained by recapturing 2 atoms after 6000 cycles. In order to estimate the efficiency of the preparation in, more specifically, the  $M = 2$  Zeeman state, we analyze the heating rate induced by the preparation light based on the following fact: an atom well prepared in state  $|\uparrow\rangle$  would not scatter photons when illuminated by the preparation light beams and would thus remain in the dipole trap unheated. Measuring the actual heating rate thus yields the probability for the atom to be in other Zeeman states of the  $F = 2$  manifold. We deduce a preparation efficiency in  $|\uparrow\rangle$  of 99.6%. To conclude on the state preparation, we can alternatively prepare the atom in the  $F = 1$  manifold (with no control over the Zeeman states) by illuminating the atom with the pumping light only.

We now turn to the state selective detection phase. At the end of the preparation stage we ramp up the trap depth to a value  $U$  and send the state detection probe light during a time  $\Delta t$ . The probe is tuned on resonance with light-shifted transition of the atom at the bottom the trap. The saturation parameter of the (unidirectional) probe is chosen sufficiently low that the effect of the potential due to the radiation pressure force is negligible on the dipole trap depth. During this probing sequence, we count the number of photons detected on the avalanche photodiode. Depending on the value of the trap depth, we adjust the duration of the probe pulse such that it induces less than 2% atom loss whilst maximizing the number of detected photons. Note that in addition to the probe induced losses, we measure an atom loss probability of 1% intrinsic to our set up, due to errors when testing for the presence of the atom at the beginning and at the end of the sequence (0.6%) and to the vacuum limited lifetime  $\tau = 23$  s of the single atom in the dipole trap (0.4%). In the results presented below we post-select the experiments where the atom is present at the end of the sequence.

The result of the experiment for a value of the trap depth of  $U = 1.4$  mK is shown in Fig. 2. This figure represents two histograms of the number  $n$  of photons detected during the probing period, for an atom pre-

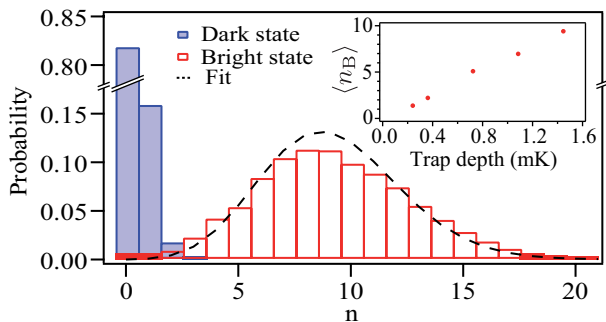


Figure 2: (Color online) Histogram of the probability to detect a number of photons  $n$  when the atom is initially prepared in the dark state (blue bars) or in the bright state (red bars). The trap depth is  $U/k_B = 1.4$  mK, the duration of the probe  $\Delta t = 1.5$  ms, and the saturation  $s = 6.1 \times 10^{-2}$ . The histograms correspond to an average of 9700 sequences. The black dashed line is a Poissonian fit to the data. (Inset) Mean number of detected photons  $\langle n_B \rangle$  versus the trap depth  $U$  for an atom prepared in the bright state.

pared respectively in the dark state (distribution  $P_D(n)$ ) and in the bright state  $|\uparrow\rangle$  (distribution  $P_B(n)$ ). In the case of the dark state the distribution is very close to Poissonian with a mean value  $\langle n_D \rangle = 0.2$  photon. We performed the same experiment when no atom is present and found no deviation with respect to the case where the atom is prepared in the dark state. The dark state signal thus comes from the background only, i.e. it corresponds to a dark count rate of the avalanche photodiode of 130 counts/sec. In the case of the preparation in  $|\uparrow\rangle$ , the histogram shows a mean number of detected photons  $\langle n_B \rangle = 9.2$  much larger than for the dark state, as expected. The distribution is also nearly Poissonian.

We also varied the trap depth and optimized the duration and the saturation parameter of the probe, as explained above. For the set of trap depths  $U/k_B = (0.24; 0.36; 0.7; 1.1; 1.4)$  mK the probe duration was respectively  $\Delta t = (0.7; 0.75; 1; 1.25; 1.5)$  ms and the saturation parameter was  $s = (1.1; 1.9; 3.7; 4.9; 6.1) \times 10^{-2}$ . The inset in Fig. 2 summarizes the results on the mean number of detected photons  $\langle n_B \rangle$  versus the trap depth  $U$  for an atom prepared in the bright state. The linear dependence indicates that the average number of photons scattered by the trapped atom varies proportionally to the trap depth, as assumed qualitatively at the beginning of this Letter. As a side result, we compare  $\langle n_B \rangle$  to the number of photons scattered by the atom during the probe pulse,  $\frac{\Gamma}{2} \frac{s}{1+s} \Delta t$ . This yields a collection efficiency of  $\approx 0.6\%$  for our imaging system, in good agreement with an independent estimate of the solid angle of the aspheric lens (7%), the transmission of the optics including the fiber coupling (20%) and the quantum efficiency of the detector (50%).

In order to characterize the performance of the state detection we use the state readout fidelity  $\mathcal{F}$  defined

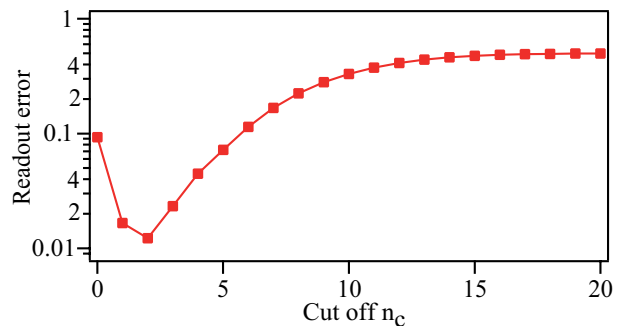


Figure 3: (Color online) Readout error  $\epsilon = 1 - \mathcal{F}$  versus the threshold on the number of detected photons,  $n_c$ , for the data of Fig. 2.

in [8]:

$$\mathcal{F} = 1 - \frac{1}{2}(\epsilon_B + \epsilon_D) \quad (1)$$

where  $\epsilon_B$  is the fraction of experiments in which an atom prepared in the bright state is detected to be dark and, conversely,  $\epsilon_D$  is the fraction of experiments where an atom prepared in the dark state is found to be bright. To calculate these quantities we define a threshold  $n_c$  on the number of detected photons. We consider that an experiment where more (resp. less) than  $n_c$  photons are detected during the probe pulse corresponds to an atom prepared in the bright (resp. dark) state. We calculate the errors  $\epsilon_B$  and  $\epsilon_D$  using

$$\epsilon_B = \sum_{n=0}^{n_c} P_B(n) \quad \text{and} \quad \epsilon_D = \sum_{n=n_c+1}^{\infty} P_D(n). \quad (2)$$

Figure 3 shows the readout error  $\epsilon = \frac{1}{2}(\epsilon_B + \epsilon_D)$  versus the threshold  $n_c$ , for the same set of data as in Fig. 2. From the data shown in Fig. 3, we extract a minimal readout error of 1.2% (obtained for  $n_c = 2$ ). This is equivalent to a state detection fidelity  $\mathcal{F} = 98.8\%$ . We repeated the same experiment 6 times over several days and found an average fidelity  $\mathcal{F} = 98.6 \pm 0.2\%$  (the error bar is statistical).

Large values of the trap depth allow us to increase the probe durations to detect more photons. As the background rate (dark count rate of the detector) remains constant, the fidelity increases, as shown in Fig. 4. We compare these data to a model using Poissonian distributions for  $P_D(n)$  and  $P_B(n)$  with mean values  $\langle n_D \rangle$  and  $\langle n_B \rangle$  that depend on the trap depth as discussed above (see inset in Fig. 2). The optimum threshold  $n_c$  is calculated for each value of the trap depth. Not surprisingly, we find good agreement between our data and the model [24].

Finally, we discuss the factors that limit our state detection fidelity to 98.6% and explore the possibilities for improvement in the future. The main contribution to the

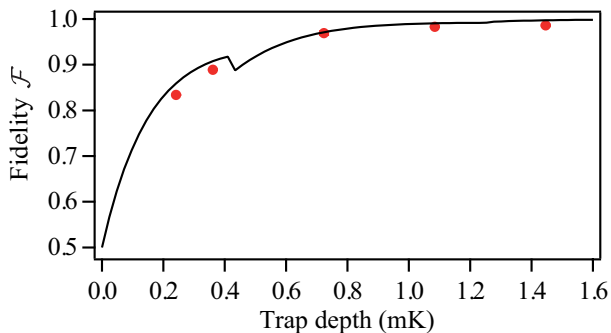


Figure 4: (Color online) State detection fidelity versus the trap depth. The black line is a model explained in the text.

error budget (see table I) comes from the dark counts of our avalanche photodiode and is  $\approx 1\%$ . Using commercially available photodiodes with a lower dark count rate of  $25 \text{ s}^{-1}$  [16] would readily bring this error contribution down to 0.3%. A small contribution to the error budget comes from the above mentioned imperfect state preparation in  $|\uparrow\rangle$  (0.03%). Off-resonant Raman transitions induced by the dipole trap light after the preparation phase also contribute for  $\approx 0.1\%$  as they mimic a bad state preparation by coupling the  $F = 1$  and  $F = 2$  levels [21]. As this contribution scales approximately as  $\Delta^{-4}$  ( $\Delta$  is the trap laser frequency detuning with respect to the fluorescence transitions), we estimate that using a trapping laser with a larger wavelength while maintaining the same trap depth would efficiently reduce this error. The last contribution, which is presently 0.27%, comes from the small number of detected photons, which leads to a small value for  $\langle n_B \rangle$  and hence to a non negligible value for  $P_B(n = 0)$ . This error will be hard to reduce significantly as  $P_B(n = 0) = e^{-\langle n_B \rangle}$  varies slowly for large values of  $\langle n_B \rangle$ .

Source of error	Contribution
Detector dark counts	1%
Detection inefficiency	0.27%
Raman transitions	0.1%
Imperfect preparation	0.03%
Total error	1.4%

Table I: Error budget of our lossless state detection.

In conclusion, we have demonstrated a lossless internal state readout of a single atom trapped in an optical tweezer. This method is based on the collection of the probe induced fluorescence using a simple imaging optics. The fidelity of the state detection is presently 98.6% in single shot, with room for technical improve-

ments in the future. Combined with our ability to efficiently control the internal states of single atoms [11, 15], this non-destructive state detection completes our toolbox for quantum engineering. We therefore believe that the detection presented in this Letter will be of great interest for future applications involving quantum measurements. Furthermore, the absence of atom loss will prevent the reloading of the atom after each measurement, thus improving the duty cycle of the experiments. It will also avoid post-detection corrections when performing quantum operations on a set of neutral atom qubits.

*Note* - During the preparation of this manuscript, we have learned of the existence of a related work [22].

We acknowledge support from the European Union through the ERC Starting Grant ARENA. A. Fuhrmanek acknowledges partial support from the DAAD Doktorandenstipendium.

- 
- [1] M.A. Nielsen and I.L. Chuang, *Quantum Computation and Quantum Information* (Cambridge University Press, Cambridge, U.K., 2000)
  - [2] T. D. Ladd, F. Jelezko, R. Laflamme, Y. Nakamura, C. Monroe, J.L. O'Brien, *Nature* **464**, 45-53 (2010).
  - [3] R. Blatt, D. Wineland, *Nature* **453**, 1008-1015 (2008).
  - [4] I. Bloch, J. Dalibard, and W. Zwerger, *Rev. Mod. Phys.* **80**, 885 (2008).
  - [5] R. Gerritsma *et al.*, *Nature* **463**, 68 (2010).
  - [6] C.F. Roos *et al.*, *Nature* **443**, 316 (2006).
  - [7] D.J. Wineland, *et al.*, *Opt. Lett.* **5**, 245 (1980).
  - [8] A. H. Myerson *et al.*, *Phys. Rev. Lett.* **100**, 200502 (2008).
  - [9] O. Mandel *et al.*, *Nature* **425**, 937 (2003).
  - [10] M. Saffman, T. G. Walker, and K. Moelmer, *Rev. Mod. Phys.* **82**, 2313 (2010).
  - [11] T. Wilk *et al.*, *Phys. Rev. Lett.* **104**, 010502 (2010).
  - [12] L. Isenhower *et al.*, *Phys. Rev. Lett.* **104**, 010503 (2010).
  - [13] S. Kuhr *et al.*, *Phys. Rev. Lett.* **91**, 213002 (2003).
  - [14] D. D. Yavuz *et al.*, *Phys. Rev. Lett.* **96**, 063001 (2006).
  - [15] M.P.A Jones *et al.*, *Phys. Rev. A* **75**, 040301 (2007).
  - [16] J. Bochmann *et al.*, *Phys. Rev. Lett.* **104**, 203601 (2010).
  - [17] R. Gehr *et al.*, *Phys. Rev. Lett.* **104**, 203602 (2010).
  - [18] B. Darquié *et al.*, *Science* **309**, 454 (2005).
  - [19] Y.R.P. Sortais *et al.*, *Phys. Rev. A* **75**, 013406 (2007).
  - [20] C. Tuchendler *et al.*, *Phys. Rev. A* **78**, 033425 (2008).
  - [21] R.A. Cline *et al.*, *Optics Letters* **19**, 207 (1994).
  - [22] M.J. Gibbons *et al.*, arXiv[quant-ph]: 1012.1682v1 (2010).
  - [23] The states  $|\downarrow\rangle$  and  $|\uparrow\rangle$  are commonly used as qubit states and can be manipulated by micro-waves [13] or Raman lasers [14].
  - [24] The discontinuities in the model are a direct consequence of  $n_c$  varying by integer values when the trap depth increases.